Journal of Membrane Science 350 (2010) 286–292

Contents lists available at ScienceDirect

Journal of Membrane Science

journal homepage: www.elsevier.com/locate/memsci

Crosslinked, epoxy-based anion conductive membranes for alkaline membrane fuel cells

Junfeng Zhou, Murat Ünlü, Irene Anestis-Richard, Paul A. Kohl*

Chemical and Biomolecular Engineering, Georgia Institute of Technology, 311 Ferst Dr, Atlanta, GA 30332-0100, USA

ARTICLE INFO

Article history:
Received 12 August 2009
Received in revised form
28 November 2009
Accepted 5 January 2010
Available online 11 January 2010

Keywords:
Crosslinked
Epoxy
Anion exchange membrane
Fuel cell

ABSTRACT

Anion conductive polysulfone membranes were successfully crosslinked via epoxy functionalities resulting in improved mechanical properties. The concentration of the epoxy crosslinker, tetraphenylolethane glycidyl ether (4EP), controlled the degree of crosslinking. All the crosslinked membranes had good thermal stability, low water uptake, low swelling, and low methanol permeability compared to non-crosslinked membranes. The crosslinked membranes showed good dimensional stability in pure methanol while non-crosslinked ones were highly soluble. Although the ionic conductivity of crosslinked membranes was slightly lower, a higher selectivity (ratio of the ionic conductivity to the methanol permeability) was obtained.

1. Introduction

Polymer electrolyte membrane fuel cells have attracted attention as an alternative energy source for transportation, portable devices, and stationary power [1,2]. Proton exchange membrane fuel cells (PEMFCs) have been extensively explored for a wide range of applications [3,4]. However, unsolved problems remain in PEMFCs including the high costs of membranes and catalysts (e.g. platinum), complex water management, and sluggish reaction kinetics [5].

Recently, anion exchange membrane fuel cells (AEMFCs), analogous to PEMFCs but operating at higher pH, have been investigated [6,7]. The high pH operation of the alkaline membrane fuel cell can potentially address many of the PEMFCs shortcomings including more facile electrokinetics, lower fuel crossover, reduced CO poisoning, and use of non-precious metal catalysts, such as silver and perovskite oxides [8]. The prospects of AEMFCs are particularly recognized for direct methanol fuel cell, which faces serious challenges with PEM-based FCs.

Anion exchange membranes (AEMs) are a key component in alkaline membrane fuel cell technology. Ions migrate from the cathode to the anode while providing a barrier to fuel crossover between the electrodes. A series of membrane materials have been reported for AEMFC applications, such as polysiloxane containing quarternary ammonium groups [9], radiation-grafted poly(vinylidene fluoride) (PVDF) [10] or poly(tetrafluoroethene-co-hexafluropropylene) (FEP) [11], quaternized poly(vinyl alcohol) (PVA) [12], quaternized poly(phthalazinon ether sulfone ketone) [13], and aminated poly(phenylene) [14].

Previous work by Zhou et al., concentrated on poly(arylene ether sulfone) membranes functionalized with quaternary ammonium groups (QAPSF) [15]. QAPSF has excellent thermal, is resistant to oxidation, and is stable under alkaline conditions (pH < 12) [16,17]. The membranes exhibited conductivities between 10 and 60 mS/cm at temperatures between 25 and 80 °C when fully hydrated in 1 M sodium carbonate [15]. In order to obtain higher conductivity aminated polysulfone membranes, a high density of quaternary ammonium groups is required. Unfortunately, a higher quaternary ammonium cation density makes the membrane susceptible to swelling by water and thus degrades performance. This challenge becomes more significant when methanol is used as the fuel. Therefore it is important to develop an AEM with sufficient cation charge density while sustaining mechanical stability, particularly in methanol.

Crosslinking has been shown to be an efficient and simple method for reducing membrane swelling and improving mechanical stability. Many strategies have been used to crosslink membranes, such as van der Waals interactions, hydrogen bonding, and ionic or covalent bonding [18]. Crosslinking via covalent bonding is the preferred method because it permanently fixes the polymer backbones. Few reports have appeared concerning covalent crosslinking of AEMs. Xu et al. prepared AEMs by thermally treating the mixture consisting of chloroacetylated poly(2,6-dimethyl-1,4-phenyleneoxide)(CPPO)/bromomethylated poly(2,6-

* Corresponding author. Tel.: +1 4048942893.
E-mail address: kohl@gatech.edu (P.A. Kohl).

0376-7388/$ – see front matter © 2010 Elsevier B.V. All rights reserved.
doi:10.1016/j.memsci.2010.01.003

dimethyl-1,4-phenylene oxide) (BPPO) [19]. A partially crosslinked structure was formed via Friedel–Crafts reaction without added crosslinker or catalyst. Wan et al. reported a crosslinked, quaternized-chitosan membrane fabricated by using glutaraldehyde as the crosslinker and sodium borohydride as the reducing agent [20].

In this report, thin polysulfone membranes were fabricated and crosslinked via thermally activated epoxy crosslinker. They have good physical and chemical stability in the presence of water and pure methanol. The thermal and electrochemical properties of these crosslinked membranes were investigated as compared with non-crosslinked polymer membranes (QAPSF).

2. Experimental

2.1. Materials and crosslinked membrane preparation

Tetraphenylolethane glycidyl ether (4EP) (Aldrich Co. Inc.), bis(4-fluorophenyl) sulphone (FPS) (Alfa Aesar Co. Inc.), 1,1,2,2-tetrachloroethane (Alfa Aesar Co. Inc.), 4,4′-(hexafluoroisopropylidene) diphenol (6F-BPA) (Alfa Aesar Co. Inc.), toluene (Alfa Aesar Co. Inc.), chloromethyl methyl ether (Aldrich Co. Inc), tin(IV) chloride (Alfa Aesar Co. Inc.), trimethylamine (Alfa Aesar Co. Inc.) and NEOSEPTA AMX (Tokuyama Corp., Japan) were used as-received. N,N-dimethylacetamide (DMAc) (Alfa Aesar Co. Inc.) was dried over 3A-molecular sieves prior to use. Potassium carbonate (Aldrich Co. Inc.) was dried at 120 °C for 24 h before polymerization. Other chemicals were of reagent grade and used as-received.

Poly(arylene ether sulfone) (PSF) terminated with phenoxide end groups was synthesized through a polycondensation reaction. The synthesis procedure is briefly described as follows [15]. A round-bottomed flask was charged with FPS, 6F-BPA (the ratio of FPS to 6F-BPA was less than one), potassium carbonate, toluene and DMAc. The mixture was stirred at room temperature for 20 min and then heated at 140 °C for 3 h and at 165 °C for 5 h under N_2 atmosphere. After the reaction, the resulting product was purified by washed with hot deionized water and ethanol several times. The chloromethylated polysulfone (CMPSF) was prepared by Friedel-Crafts electrophilic substitution reaction under anhydrous conditions at 120 °C using PSF as the starting material, and chloromethyl methyl ether as the chloromethyl reagent. Different amounts of 4EP (1.0 and 3.0 wt%, with respect to the CMPSF weight) were added to CMPSF/DMAc solution. The resulting mixtures were stirred for 12 h and filtered to remove particles. The solution was cast onto Teflon plates. The films were formed at 50 °C for 12 h to evaporate the solvent. The samples were cured by slowly raising the temperature to 160 °C and holding for 3 h in a nitrogen atmosphere to achieve crosslinking. The resulting membranes were immersed in aqueous trimethylamine (45%, w/w) for 5 days to convert the chloride sites into benzyl trimethylammonium cation groups. The non-crosslinked membranes (QAPSF) were prepared as described previously [15] as a control.

2.2. Structural characterization

FT-IR absorption spectra were recorded using a Nicolet Magna 560 FT-IR spectrometer. The FT-IR samples were made by casting films on KBr plates from a DMAc solution. The samples were dried in nitrogen and analyzed in transmission mode.

Thermogravimetry analysis (TGA) was carried out in flowing nitrogen (60 cm^3/min) using a TA Q50 thermal analyzer. Samples were heated from ambient temperature to 800 °C at a heating rate of 1.0 °C/min.

The ^1H NMR spectra of the synthesized polymers were recorded for structural characterization. Data were collected with a Model DMX400 spectrometer using chloroform-d solutions.

2.3. Ion exchange capacity (IEC), water uptake and swelling ratio

The ion exchange capacity of these membranes was measured using the classical titration method [21]. The membranes were immersed in a large volume of 0.1 M NaOH solution to convert them from the chloride-form to the hydroxide form. They were then rinsed with deionized water to remove excess NaOH. The hydroxide was neutralized by immersing the samples in 50 mL of 0.1 M HCl solution for 24 h. The IEC was determined by titration of the HCl solution to measure the amount of acid neutralized by the hydroxide. The IEC milliequivalents per gram (meq/g) was obtained from Eq. (1):

$$\mathrm{IEC\,(meq/g)} = \frac{M_o - M_e}{m_d} \tag{1}$$

where M_o is the milliequivalents (meq) of HCl measured before membrane neutralization, M_e is the meq of HCl measured after neutralization, and m_d is the mass (g) of the dried membrane.

The water uptake and swelling of the membranes were evaluated by first drying the films in a desiccator over anhydrous calcium chloride at ambient temperature until constant dry weight (W_d) and length (L_d) were obtained [22]. The dry membranes were immersed in deionized water at different temperatures for 24 h. The surface water was swabbed away with tissue paper before weighing. The weight and length were measured several times until constant weight (W_w) and length (L_w) were achieved. The water uptake of membranes was calculated using Eq. (2):

$$\mathrm{Water\ uptake\,(\%)} = \left[\frac{W_w - W_d}{W_d}\right] \times 100\% \tag{2}$$

The swelling ratio of membranes was calculated using Eq. (3):

$$\mathrm{Swelling\ ratio\,(\%)} = \left[\frac{L_w - L_d}{L_d}\right] \times 100\% \tag{3}$$

2.4. Ionic conductivity

The ionic conductivity of the membranes was measured with a four-electrode ac impedance method using a frequency response analyzer (PAR 2273 potentiostat/galvanostat, Princeton Applied Research) from 1 Hz to 2 MHz. All membranes in the carbonate-form were initially hydrated by immersing in deionized water at room temperature for 24 h before measurement. The 1 M Na_2CO_3 solution resistance ($R_{solution}$) (without the membrane present) was measured in a conductivity glass cell to obtain the cell constant. The fully hydrated membrane was placed in the middle of the conductivity glass cell and the cell resistance (R_{total}) of the solution and membrane was measured. The membrane resistance (R) was obtained the difference between the two measured resistances ($R_{solution}$ and R_{total}). Conductivity measurements were carried out from 25 to 80 °C. The conductivity (σ) of the membranes was calculated using the following Eq. (4):

$$\sigma = \frac{L}{RA} \tag{4}$$

where L, R, and A denote the thickness of the membrane, the membrane resistance, and the cross-sectional area of the membrane exposed to the solution, respectively.

2.5. Methanol permeability [23]

The methanol permeability of the membranes was measured by Gasa's method. 20-mL glass vials were filled with 10 mL pure

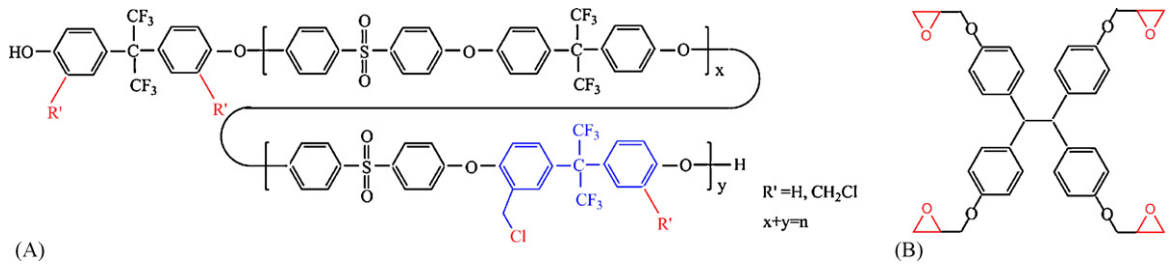

Fig. 1. Chemical structures of CMPSF (A) and 4EP (B).

methanol. The membranes were clamped between the mouth of the vial and the cap. The cap had a 3.5 mm hole so that the methanol could escape only through the hole. The mass of the methanol inside the cell was measured as a function of time at room temperature. The methanol permeability (P) was calculated by Eq. (5):

$$P = \frac{N \times l}{\Delta P \times A \times t} \quad (5)$$

where N is the number of moles of methanol lost (moles), l is the thickness of the membrane (cm), ΔP is the saturated vapor pressure of methanol (16,077 Pa), A is the area of the small hole on the cap (cm^2), and t is the time (days).

3. Results and discussion

3.1. Synthesis and characterization of crosslinked-epoxy-based electrolyte membrane

A series of poly(arylene ether sulfone) polymers terminated with phenoxide end groups were synthesized through a polycondensation reaction from 6F-BPA and FPS by nucleophilic aromatic substitution. 6F-BPA was used in excess to end-cap the copolymers with the phenoxide groups, so that the phenoxide groups could be further reacted in the crosslinking step. The chloromethylated poly(arylene ether sulfone) (CMPSF) (Fig. 1A) was prepared by a Friedel-Crafts electrophilic substitution reaction. The degree of chloromethylation in the resulting product was controlled by varying the reaction time, which affected the ultimate conductivity of these anion exchange membranes [15]. CMPSF was initially crosslinked by mixing with different amounts of 4EP (Fig. 1B) (CMPSF/4EP) and curing at elevated temperatures for 3 h in a nitrogen atmosphere. The crosslinked CMPSF/4EP membranes were transformed into the quaternary amino base by immersing the membranes in a solution consisting of 45% trimethylamine at ambient temperature for 5 days. Notably, poly(arylene ether sulfone) functionalized with quaternary ammonium groups was not used as the starting material for the crosslinking reaction since the quaternary ammonium groups started to decompose at high temperature (i.e. >160 °C) in nitrogen atmosphere. The crosslinking of the membranes were qualitatively tested by observing dimensional stability in pure methanol. When the curing temperature was 130 °C, the samples dissolved in neat methanol indicating that the degree of crosslinking was incomplete. When the membrane was cured at 160 °C, it was dimensionally stable in pure methanol. The membrane changed color from brownish-yellow to dark-brown when heated. Similar observations were made for the crosslinking of sulphonated poly(ether ether ketone) using aromatic bis(hydroxymethyl) compound [24].

FT-IR spectroscopy was used to confirm the crosslinking reaction between the epoxide and phenoxide groups. The FT-IR spectra of uncured CMPSF/4EP, as well as a thermally cured membrane, are shown in Fig. 2. Compared to the uncured membrane, the peak height for the epoxy deformation (926 cm^{-1}) decreased in thermally cured membrane while other characteristic peaks remained the same [25]. It shows that the epoxide ring opened and generated hydroxyl groups which can react with the phenoxide groups to produce a three-dimensional epoxy network [26].

The formation of quaternary ammonium groups within the crosslinked membranes (CMPSF/4EP) was also confirmed by FT-IR. As shown in Fig. 3A, the peaks at 1587, 1509, and 1489 cm^{-1} are due to the skeletal vibration of the aromatic hydrocarbons. The peak at 1246 cm^{-1} is assigned to the antisymmetric vibration of the ether linkage. The characteristic peaks at 1205 and 1020 cm^{-1} are due to the symmetric and asymmetric stretching of the S=O bond. The peak for the $-CH_3$ stretch at 3005 cm^{-1} (Fig. 3B) increased in height after the quaternary ammonium cation was formed due to the addition of the methyl group. The results show that the quaternary ammonium groups were indeed attached to the copolymer backbone.

3.2. Thermal stability

The thermal stability of the polymer electrolyte is a key metric for fuel cell use. The thermal decomposition of the synthesized non-crosslinked and crosslinked membranes in the chloride-form was evaluated via TGA. The heating rate was 1.0 °C/min in a nitrogen atmosphere, unless otherwise stated. The samples were dried in a vacuum oven overnight at 100 °C prior to thermal analysis. Figs. 4 and 5 shows the TGA and differential gravimetric analysis (DGA), respectively, for the non-crosslinked membrane (N0) and crosslinked membrane (N2). The initial weight loss of the chloride-loaded membranes (25–194 °C) is attributed to the loss of residual solvent (DMAc) and water. There are three additional

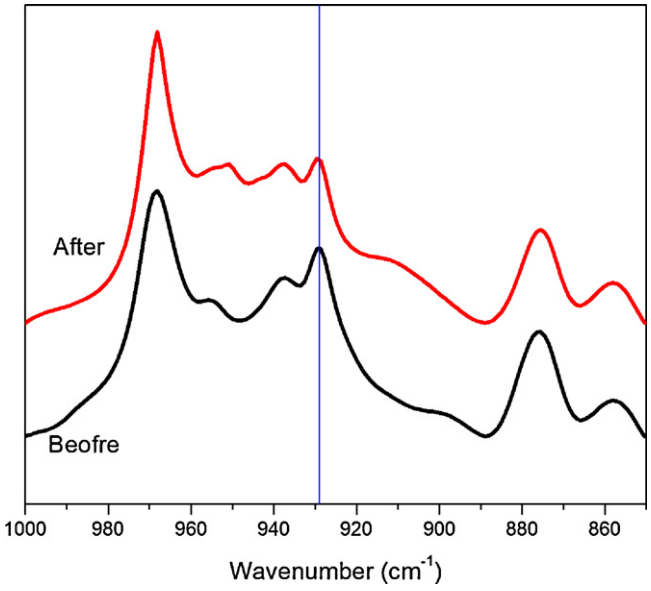

Fig. 2. Comparison of the FT-IR spectra of before and after thermally cured CMPSF/4EP membranes.

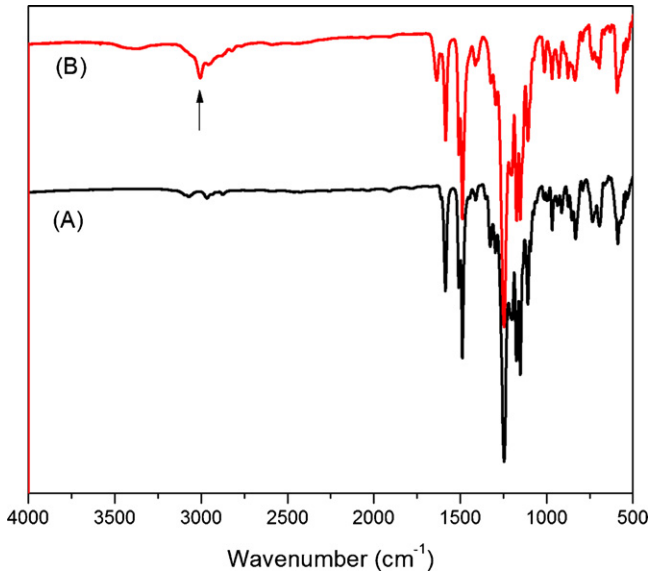

Fig. 3. FT-IR spectra of crosslinked CMPSF/4EP (A) and aminated crosslinked (B) membranes.

principal weight loss regions corresponding to peaks in the DTG. The first region (ca. 259 °C) is due to the degradation of the quaternary ammonium groups grafted to the polymer backbone. The total weight loss at this stage in the TGA is about 17%. The second region is at 354 °C and is due to the degradation of the polymer chains. The total weight loss is about 33%. The third region occurs at 482 °C and leads to the polymer backbone cleavage. The total weight loss is about 51%. The TGA and DGA curves for non-crosslinked and crosslinked membranes were very similar except in the quaternary ammonium degradation region. The degradation of quarternay ammonium groups in the crosslinked membrane at ca. 200 °C is slightly greater than that in the non-crosslinked membrane. Thus, the degradation peak of the crosslinked sample is shifted slightly toward higher temperature which is likely due to the 4EP crosslinker additive. These results show that the dry, crosslinked electrolyte membrane is thermally stable to about 200 °C.

Here, for future direct comparisons with the crosslinked and non-crosslinked membranes, commercial AEM membrane (Tokuyama AMX) was also measured at the same condition.

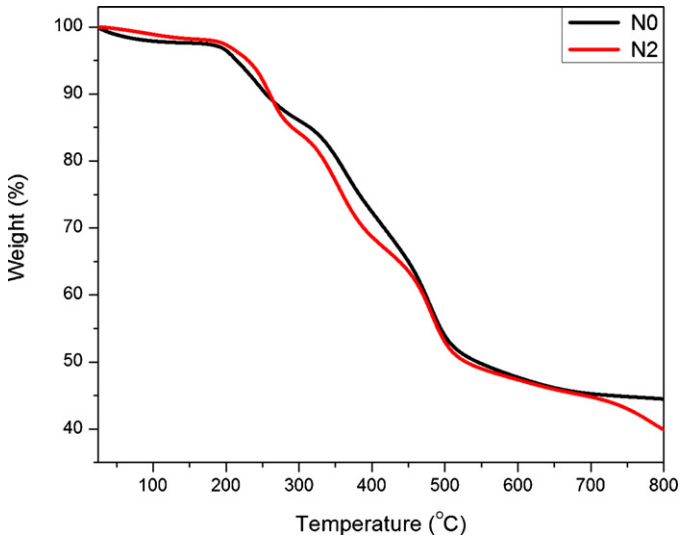

Fig. 4. TGA curves of non-crosslinked (N0) and crosslinked membranes (N2) in nitrogen.

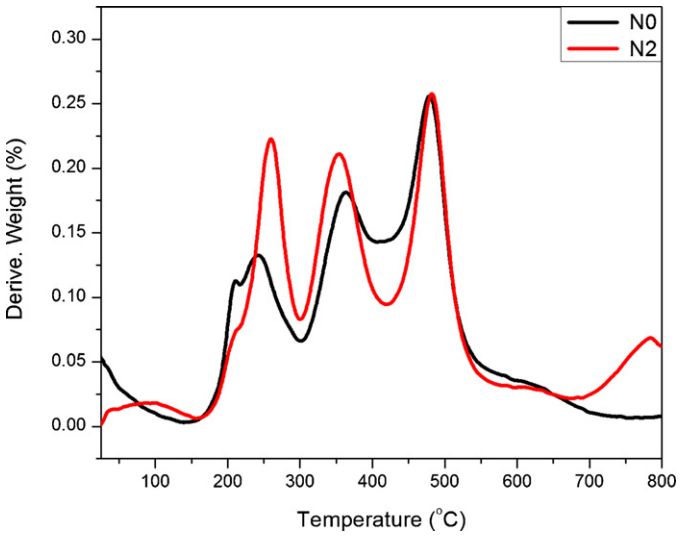

Fig. 5. DGA curves of non-crosslinked (N0) and crosslinked membranes (N2) in nitrogen.

3.3. Ion exchange capacity, water uptake and swelling ratio

Ion exchange capacity (IEC) as measured in meq/g, is an important factor in determining the performance of AEMs. It provides information on the density of the fixed cation sites in the membrane [21]. The IEC of each membrane was evaluated by acid-base titration, as described above. The results are listed in Table 1. However, the values were lower than the cation values estimated from ^{1}H NMR data. It can be seen that there is a gradual decrease in IEC with an increase in the degree of crosslinking.

The water uptake of polymer electrolyte is generally observed to have a profound effect on ionic conductivity and mechanical property. Membranes with low water uptake typically show low ionic conductivity. The mechanical strength is generally compromised in membranes with high water uptake. Consequently, water management is a critical factor in optimizing fuel cell operation. As a result, the degree of water uptake in water was characterized for the non-crosslinked, crosslinked and AMX membranes in the carbonate-form as a function of temperature.

Fig. 6 shows the percent water uptake in water as a function of temperature. The water uptake of these membranes, except the non-crosslinked N0 sample and AMX membrane, increased moderately as a function of temperature from 25 to 60 °C at which point the uptake increased dramatically. Above 70 °C, the membranes absorbed an excessive amount of water. This indicates that the water uptake strongly depends on the density of the quaternary

Table 1
The degree of chloromethylation and membrane IEC.

Sample	4EP content (wt%)	DC[a]	IEC (meq/g)[b]	IEC (meq/g)[c]
M0	0	1.21	1.83	1.31
M1	1	–	–	1.19
M2	3	–	–	0.73
N0	0	1.45	2.18	1.63
N1	1	–	–	1.36
N2	3	–	–	0.87
AMX				1.4–1.7

[a] Degree of chloromethylation = (number of chloromethyl groups/repeat unit), calculated from ^{1}H NMR spectra.
[b] Theoretical IEC calculated from ^{1}H NMR.
[c] Calculated from titration data.

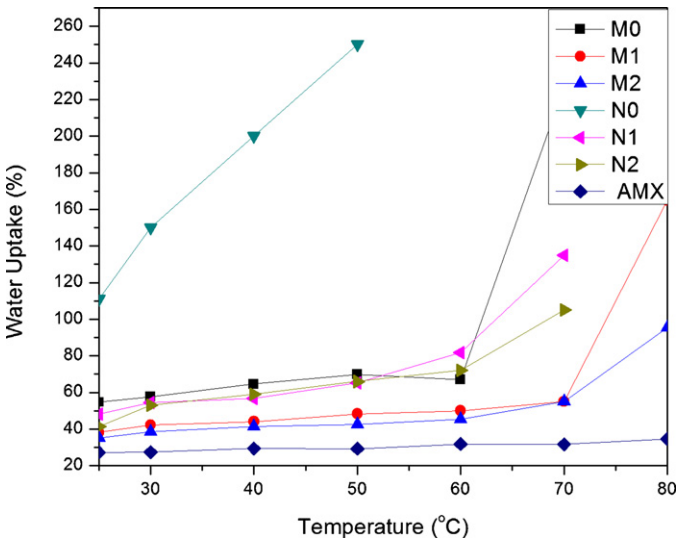

Fig. 6. Temperature dependence of water uptake of the different membranes.

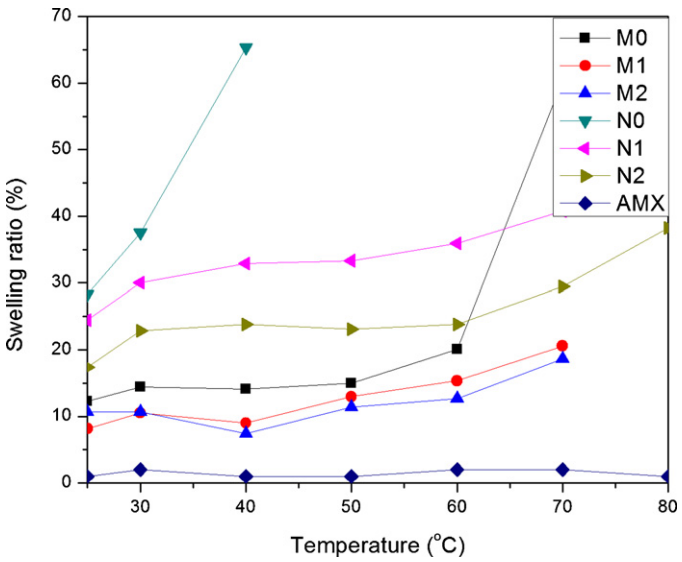

Fig. 7. Temperature dependence of swelling ratio of the different membranes.

ammonium sites and the temperature. Higher temperature results in a higher degree of hydrophilicity from the quaternary ammonium cations [27]. The non-crosslinked membrane, N0, had a high value for IEC and considerable swelling, resulting in poor mechanical strength at high temperature. At 60 °C, the membrane dissolved in the hot water after 24 h. However, AMX membrane here shows constant water uptake (around 30.0 wt%) at different temperature.

It also can be seen that the non-crosslinked membranes (M0 and N0) exhibit higher water uptake than the crosslinked ones (M1, M2, N1, N2). Especially comparing M0 and M2, the water uptake decreased from 225 to 50 wt%. This decrease in water uptake is the direct effect of crosslinking. The crosslinking increases the interaction of the polymers, hinders chains mobility and forms condense network between the polymer chains [28], which results in lower water uptake. The higher 4EP content results in a more compact structure, and restricts the mobility of polymer chains which could decrease the uptake of water in the membranes [29].

The ratio of the volume of the swollen to unswollen membrane, swelling ratio, is an important property for fuel cell operation because it affects the dimensional stability of the membrane. If the swelling ratio is too large, it will cause a dimensional mismatch or weakness between the electrode and the membrane in membrane electrode assembly (MEA). Consequently, a dimensionally stable membrane with adequate water uptake and lowest swelling is needed for AEMFCs. The swelling ratio of the membranes in carbonate-form was measured in pure water as a function of temperature. The swelling ratio of the non-crosslinked, crosslinked and AMX membranes is shown in Fig. 7. AMX membrane almost did not change anything in size due to the fabric support. The crosslinked and non-crosslinked membranes follow the same trend as the water uptake in Fig. 6. The crosslinked membranes show less swelling than the non-crosslinked samples. For example, the swelling ratio decreased from 65% to 22% at 40 °C by crosslinking sample M0, as shown in sample M2. Crosslinking restrains the movement of polymer chains, improving the dimensional stability.

3.4. Ionic conductivity and methanol permeability

The ionic conductivity of the membranes is of particular importance and plays a significant role in fuel cell performance. IR loss within the membrane lowers the overall conversion efficiency within the fuel cell. The conductivity of the carbonate ion within the fuel cell was as a figure of merit for relative conductivity because hydroxide can degrade the membrane conductivity, especially at higher temperature. Hydroxide is an aggressive nucleophile and can result in loss of cations within the membrane [15]. In this study, the carbonate-loaded membranes were initially hydrated by immersion in deionized water for 24 h at room temperature before ionic conductivity measurements. The hydrated membrane resistance, thickness and diameter were measured as a function of temperature and used to calculate the ionic conductivity. The ionic conductivity of the non-crosslinked, crosslinked and AMX membranes in the carbonate-form as a function of the temperature is shown in Fig. 8. The ionic conductivity of the samples was about 0.01 S/cm at 30 °C except sample M2 and AMX which had the lower IEC. The ionic conductivity increased with temperature regardless of the 4EP content. This is due to higher diffusivity as the temperature is raised and more water is absorbed by the membranes [30].

The crosslinked membranes, except sample M2, had higher conductivity than the commercial membrane (AMX). While the crosslinked membranes had slightly lower conductivity compared to the responding non-crosslinked membranes. Further, there is a slight descending trend with 4EP content. For example, the

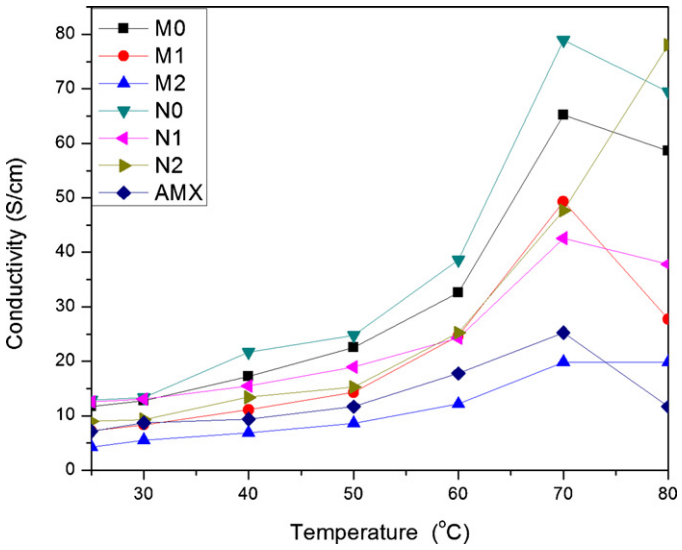

Fig. 8. Temperature dependence of the ionic conductivity of the different membranes.

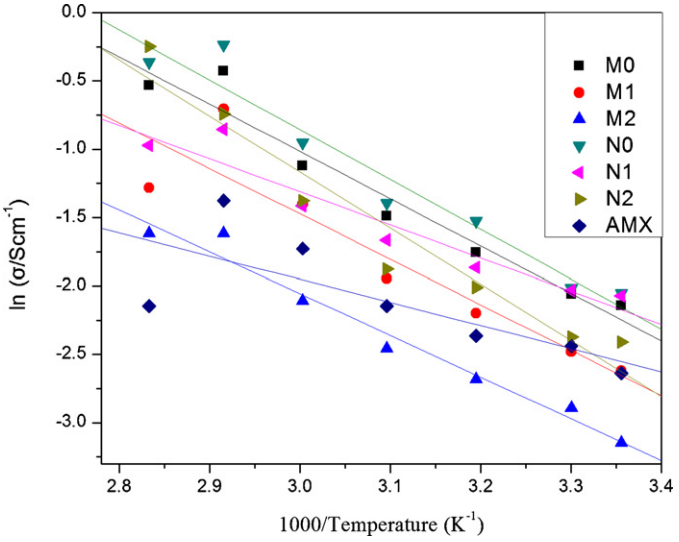

Fig. 9. The $\ln\sigma$ vs. $1000/T$ plot for the different membranes; the lines indicate the linear regression.

uncrosslinked membrane M0 had a conductivity of 12.75 mS/cm at 30 °C, whereas the crosslinked versions, M1 and M2, had conductivities of 8.37 and 5.53 mS/cm, respectively, under the same conditions. The decrease in ionic conductivity could be the result of: (1) the decrease concentration of charge carriers in the membranes with the addition of 4EP; or (2) the crosslinking structure restricts the mobility of charged sites and decreases the free volume of these membranes, which may result in less and smaller hydrophilic pathway for carbonate mobility [29].

The activation energy for ion-migration, E_a, was estimated from Fig. 9. Linear regression of natural log of conductivity vs. $1/T$ was performed assuming an Arrhenius relationship. The ion transport activation energy, E_a, for the membranes was calculated using Eq. (6) [12]:

$$E_a = -b \times R \quad (6)$$

where b is the slope of the line regression of $\ln\sigma$ (S/cm) vs. $1000/T$ (K^{-1}) plots, and R is the gas constant (8.31 J K^{-1} mol^{-1}).

The E_a of the non-crosslinked, crosslinked and AMX membranes were between 14.04 and 34.08 kJ/mol, which is higher than the E_a of Nafion 115 (6.00 kJ/mol) as reported by Slade and co-worker [31]. It demonstrates that carbonate ion mobility in these membranes is more difficult than protons in Nafion, and more sensitive to temperature. This is likely due to the larger size of carbonate ions than that of hydrated protons [15].

AEMs used in fuel cell applications should have high ionic conductivity and be an effective barrier for reactant crossover. Methanol permeability through the non-crosslinked, crosslinked and AMX membranes was measured as a metric of reactant crossover by using pure methanol at room temperature, as calculated using Eq. (5). For comparison, the methanol permeability of Nafion 117 was also measured at the same conditions. The relative data are shown in Fig. 10. The permeability of the non-crosslinked membrane could not be measured since the membranes dissolved in methanol. The methanol permeability of the crosslinked membranes was lower than that of AMX and Nafion 117. The membranes crosslinked here formed more compact microstructures than AMX and Nafion resulting in lower methanol permeability [27]. It also can be seen that the methanol permeability of the crosslinked membranes increased with 4EP content and followed the IEC trends.

Selectivity factor, which is the ratio of the ionic conductivity to the methanol permeability, is often used to evaluate the potential

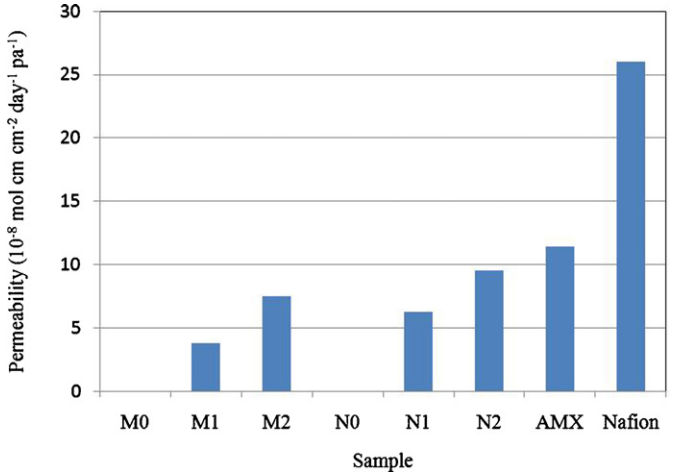

Fig. 10. Methanol permeability of different membranes at room temperature.

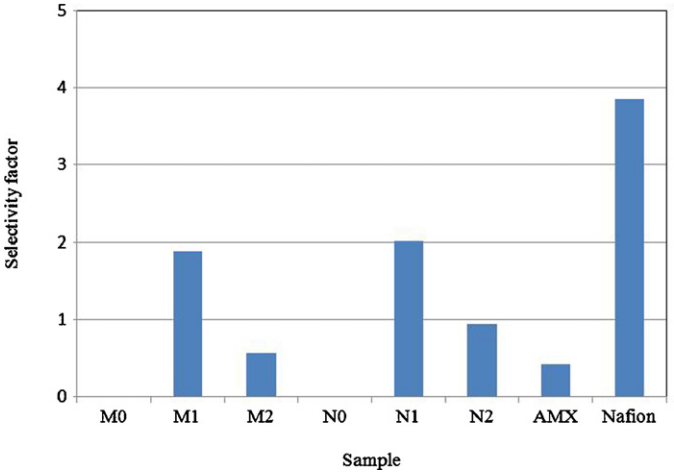

Fig. 11. Selectivity factor of different membranes at room temperature.

of applications as the ion exchange membranes in direct methanol fuel cells [32,33]. The relative selectivity of the crosslinked membranes synthesized here is shown in Fig. 11. Those values are lower than Nafion 117, while they are much higher than AMX. Consequently, the crosslinked membranes have the potential to replace AMX membrane in AEMFC applications. The higher conductivity of Nafion (proton exchange membrane) out-weighs its higher permeability. Thus, further improvements in ionic conductivity are needed in anion exchange membranes. Sample N1 showed the best selectivity for the membranes studied here due to its relatively low methanol permeability and high ionic conductivity. The small decrease of methanol permeability for the crosslinked membrane more than compensates for the decrease in ionic conductivity.

4. Conclusion

A series of novel crosslinked polysulfone membranes were successfully prepared and crosslinked using 4EP. The crosslinking and amination reactions were verified by FT-IR. Although the crosslinking slightly reduced the ionic conductivity of polysulfone membranes compared to the non-crosslinked membrane, the water uptake, swelling, and methanol permeability were reduced significantly. The crosslinked membrane (N1) prepared here was offered the best combination of conductivity, low methanol permeability, swelling resistance, and thermal stability. In addition, the results show that crosslinking via epoxy groups is an effective

method to decrease the water uptake, methanol permeability, and increases the dimension stability without excessive loss of ionic conductivity. Significantly, these crosslinked membranes showed good mechanical stability in pure methanol while non-crosslinked ones were highly soluble.

References

[1] J.H. Chen, M. Asano, Y. Maekawa, M. Yoshida, J. Polym. Sci. Polym. Chem. 46 (2008) 5559–5567.
[2] D.S. Kim, Y.S. Kim, M.D. Guiver, B.S. Pivovar, J. Membr. Sci. 321 (2008) 199–208.
[3] P. Jain, L.T. Biegler, M.S. Jhon, AIChE J. 54 (2008) 2089–2100.
[4] Y.Z. Fan, H.Q. Hu, H. Liu, J. Power Sources 171 (2007) 348–354.
[5] V. Rao, C. Cremers, U. Stimming, Fuel Cells 5 (2007) 417–423.
[6] J.R. Varcoe, R.C.T. Slade, E. Lam How Yee, S.D. Poynton, D.J. Driscoll, D.C. Apperley, Chem. Mater. 19 (2007) 2686–2693.
[7] J.R. Varcoe, R.C.T. Slade, E. Lam How Yee, Chem. Commun. (2006) 1428–1429.
[8] K. Matsuoka, S. Chiba, Y. Iriyama, T. Abe, M. Matsuoka, K. Kikuchi, Z. Ogumi, Thin Solid Films 516 (2008) 3309–3313.
[9] J.J. Kang, W.Y. Li, Y. Lin, X.P. Li, X.R. Xiao, S.B. Fang, Polym. Adv. Technol. 15 (2004) 61–64.
[10] L. Li, Y.X. Wang, J. Membr. Sci. 262 (2005) 1–4.
[11] R.C.T. Slade, J.R. Varcoe, Solid State Ionics 176 (2005) 585.
[12] Y. Xiong, J. Fang, Q.H. Zeng, Q.L. Liu, J. Membr. Sci. 311 (2008) 319–325.
[13] J. Fang, P.K. Shen, J. Membr. Sci. 285 (2006) 317–322.
[14] T.S. Olson, E.E. Switzer, P. Atanassov, M.R. Hibbs, C.J. Cornelius, 211th ECS Meeting, abstract #282.
[15] J.F. Zhou, M. Unlu, J.A. Vega, P.A. Kohl, J. Power Sources 190 (2009) 285–292.
[16] B.R. Einsla, E. McGrath, J. Am. Chem. Soc. Div. Fuel Chem. 49 (2004) 616–618.
[17] B. Lafitte, M. Puchner, P. Jannasch, Macromol. Rapid Commun. 26 (2005) 1464–1468.
[18] M. Paul, H.B. Park, B.D. Freeman, A. Roy, J.E. McGrath, J.S. Riffle, Polymer 49 (2008) 2243–2252.
[19] L. Wu, T.W. Xu, J. Membr. Sci. 332 (2008) 286–292.
[20] Y. Wan, B. Peppley, K.A.M. Creber, V.T. Bui, E. Halliop, J. Power Sources 185 (2008) 183–187.
[21] Y. Xiong, Q.L. Liu, A.M. Zhu, S.M. Huang, Q.H. Zeng, J. Power Sources 186 (2009) 328–333.
[22] H. Herman, R.C.T. Slade, J.R. Varcoe, J. Membr. Sci. 218 (2003) 147–163.
[23] J.V. Gasa, R.A. Weiss, M.T. Shaw, J. Membr. Sci. 304 (2007) 173–180.
[24] V.R. Hande, S. Rao, S.K. Rath, A. Thakur, M. Patri, J. Membr. Sci. 322 (2008) 67–73.
[25] X.J. Duthie, S.E. Kentish, C.E. Powell, G.G. Qiao, K. Nagai, G.W. Stevens, Ind. Eng. Chem. Res. 46 (2007) 8183–8192.
[26] C.H. Lee, Y.Z. Wang, J. Polym. Sci. Polym. Chem. 46 (2008) 2262–2276.
[27] T.Z. Fu, S.L. Zhong, Z.M. Cui, C.J. Zhao, Y.H. Shi, W.Z. Yu, H. Na, W. Xing, J. Appl. Polym. Sci. 111 (2009) 1335–1343.
[28] J.H. Pang, H.B. Zhang, X.F. Li, D.F. Ren, Z.H. Jiang, Macromol. Rapid Commun. 28 (2007) 2332–2338.
[29] S.G. Feng, Y.M. Shang, X.F. Xie, Y.Z. Wang, J.M. Xu, J. Membr. Sci. 335 (2009) 13–20.
[30] P.L. Kuo, W.J. Liang, C.Y. Hsu, W.H. Jheng, Polymer 49 (2008) 1792–1799.
[31] M. Saito, K. Hayamizu, T. Okada, J. Phys. Chem. B 109 (2005) 3112–3119.
[32] D.S. Kim, G.P. Robertson, M.D. Guiver, Macromolecules 42 (2009) 957–963.
[33] S. Prakash, W. Mustain, P.A. Kohl, Electrolytes for Long-Life, Ultra Low-Power Direct Methanol Fuel Cells in Advances in Fuel Cells, Elsevier, 2008.